

AD-A147 962

RUBBER-MODIFIED EPOXIES II MORPHOLOGY TRANSITIONS AND
MECHANICAL PROPERTIES(U) PRINCETON UNIV NJ DEPT OF
CHEMICAL ENGINEERING L C CHAN ET AL. NOV 84

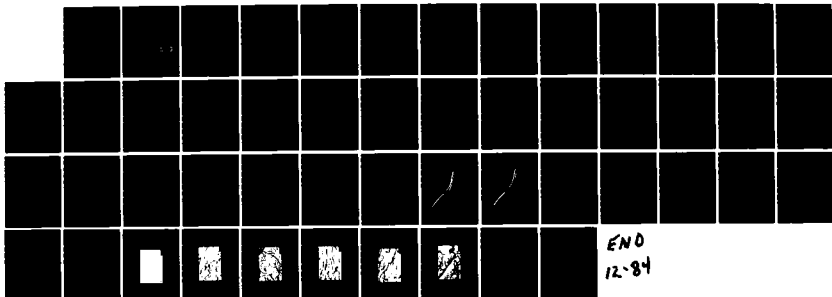
1/1

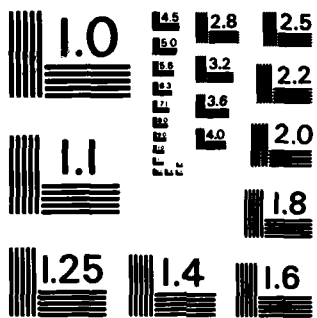
UNCLASSIFIED

N00014-84-K-0021

F/G 11/10

NL





MICROCOPY RESOLUTION TEST CHART
NATIONAL BUREAU OF STANDARDS - 1963 - A

12

OFFICE OF NAVAL RESEARCH

Contract N00014-84-K-0021

TECHNICAL REPORT NO. 3

AD-A147 962

RUBBER-MODIFIED EPOXIES:

II. MORPHOLOGY, TRANSITIONS, AND MECHANICAL PROPERTIES

by

L. C. Chan, J. K. Gillham, A. J. Kinloch and S. J. Shaw

for publication in

Advances in Chemistry Series, Number 209
American Chemical Society
Washington, D.C.

PRINCETON UNIVERSITY
Polymer Materials Program
Department of Chemical Engineering
Princeton, New Jersey 08544

DTIC
ELECTE
NOV 15 1984
S B D

November 1984

Reproduction in whole or in part is permitted for
any purpose of the United States Government

This document has been approved for public release and sale;
its distribution is unlimited

Principal Investigator
John K. Gillham
(609) 452-4694

84 11 2 012

DTIC FILE COPY

UNCLASSIFIED

SECURITY CLASSIFICATION OF THIS PAGE(When Data Entered)

phase and the inherent ductility of the matrix, the latter being related to
E^T g[∞]

UNCLASSIFIED

SECURITY CLASSIFICATION OF THIS PAGE(When Data Entered)

RUBBER-MODIFIED EPOXIES:

II. MORPHOLOGY, TRANSITIONS, AND MECHANICAL PROPERTIES

L. C. Chan and J. K. Gillham
Polymer Materials Program
Department of Chemical Engineering
Princeton University
Princeton, NJ 08544 U.S.A.

and

A. J. Kinloch and S. J. Shaw
Ministry of Defence
Royal Armament Research and Development
Establishment (Waltham Abbey)
Essex EN9 1BP U.K.

G sub IC

ABSTRACT

glass transition temperature

The mechanical properties of two fully cured rubber-modified epoxy systems, each with varying morphologies and maximum glass transition temperatures ($T_{g\infty}$) developed from different cure conditions, have been investigated versus temperature (-90 to 140°C) using the neat system ($T_{g\infty} = 167^\circ\text{C}$) as control. The mechanical properties of the amino-terminated rubber-modified system were more sensitive to cure history than those of the prereacted carboxyl-terminated rubber-modified system. The improvement of fracture energy (G_{IC}) at a low strain rate for a rubber-modified epoxy system depends on both the volume fraction of the dispersed phase and the inherent ductility of the matrix, the latter being related to $T_{g\infty}$.



Accession For	
NTIS GRA&I	<input checked="" type="checkbox"/>
DTIC TAB	<input type="checkbox"/>
Unannounced	<input type="checkbox"/>
Justification	
By _____	
Distribution/	
Availability Codes	
Dist	Special
A-1	

INTRODUCTION

The crack resistance of cured, brittle epoxy materials can be improved by addition of reactive liquid rubber to the uncured epoxy formulations (1,2). A cured rubber-modified material usually exhibits a two-phase structure consisting of finely dispersed rubber-rich domains ($\sim 0.1 - 5 \mu\text{m}$) bonded to the epoxy matrix. The mechanical properties are dependent on the relative amounts of dissolved and phase-separated rubber, the domain size and size distribution of the dispersed phase, and the chemical and physical compositions of the matrix and of the dispersed phase (3-8).

In the previous paper (9), the cure process and its relationship to the development of morphology and transitions for two rubber-modified epoxy systems was discussed. In an attempt to develop and arrest a fully cured but distinct cure-dependent morphology, a two-step cure process was used: a) the resin was cured isothermally at different temperatures (T_{cure}) until reactions ceased, and b) the cured resin was postcured by heating above the maximum glass transition temperature ($T_{\text{g}\infty}$) of the system to complete the reactions of the matrix. A tetrafunctional aromatic diamine-cured diglycidyl ether of bisphenol A (DGEBA)-type epoxy resin was selected as the neat system because of its high $T_{\text{g}\infty}$ (167°C). The two rubber-modified systems containing 15 phr of rubber were obtained by modifying the neat system with a commercial prereacted carboxyl-terminated rubber and a commercial amino-terminated rubber, respectively; both rubbers had been made from the same copolymer of butadiene and acrylonitrile.

The main objective of this research was to investigate the mechanical properties of fully cured specimens of the two rubber-modified epoxy systems, each

with varying morphologies and maximum glass transition temperatures which had been made using different cure conditions, with the neat system as the control. Dynamic mechanical properties in torsion, uniaxial compressive modulus, yield stress and strain behavior, and tensile fracture behavior at a low strain rate were obtained over a range of test temperatures (-90 to 140°C).

EXPERIMENTAL

Materials

The chemical structures of the materials used for the neat and the two rubber-modified systems have been described in the previous paper (9). The neat system was a DGEBA-type epoxy resin (DER 331, Dow Chemical Co.) cured with trimethylene glycol di-p-aminobenzoate ("TMAB", i.e. Polacure 740M, Polaroid Corp.). The first system, denoted DTK-293, was modified with a commercial prereacted carboxyl-terminated butadiene-acrylonitrile copolymer ("K-293", Spencer Kellog Co.). The K-293 rubber had been made by reacting a carboxyl-terminated rubber containing 17% acrylonitrile (CTBNx8, B. F. Goodrich Chemical Co.) with excess of DGEBA resin. The second system, denoted DTAx16, was modified with a commercial amino-terminated butadiene-acrylonitrile copolymer also containing 17% acrylonitrile (ATBNx16, B. F. Goodrich Chemical Co.). The commercial ATBN rubber contained a residual amount (~3% by weight) of N-(2-aminoethyl) piperazine (AEP) from its synthesis (10). The formulations for the neat and the two rubber-modified systems, each containing 15 phr of the butadiene-acrylonitrile copolymer, are included in Table I. The neat epoxy system was also modified with 15 phr of the unreacted carboxyl-

terminated rubber (CTBNx8) in an attempt to investigate the effect of poor interfacial bonding on fracture behavior.

Specimen Preparation

The mixture of liquid epoxy resin and liquid rubber (for the modified systems) was heated to 120°C in an open beaker and the solid curing agent was added and dissolved with the aid of mechanical stirring for 5 minutes. The solution was degassed at 100°C for 25 minutes in a preheated vacuum oven at a pressure of about 1 torr, and then was poured into two preheated (at T_{cure}) molds [pre-coated with a release agent (QZ13, Ciba-Geigy Chemical Co.) (11)], and cured according to the chosen cure conditions (Table II) to form a large casting for the compact tension and film specimens, and small rods for the compression specimens, respectively. The large casting (220x220x6 mm) was prepared in an air oven, the open end of the mold being sealed with a plug made of silicone rubber (RTV660, General Electric Co.) to minimize exposure to air during cure. The rods (length \approx 60 mm, diameter = 7 mm) were prepared under nitrogen in an oven. After cure, the molds were allowed to cool freely inside the ovens to room temperature (\sim 1°C/minute). The casting and rods were then removed from their molds, and specimens were machined to the specified dimensions for mechanical testing. Residual stresses were removed by an annealing process in nitrogen which involved heating the specimens from room temperature to 200°C before freely cooling them to room temperature.

Transmission Electron Microscopy (TEM)

Morphologies of cured specimens were examined using TEM micrographs (9). Specimens (from previously fractured compact tension specimens) were stained with osmium tetroxide (which reacted with the double bonds of the rubber) and were microtomed at room temperature. The volume fraction and mean diameter of the dispersed phase were determined by using both Schwartz-Saltykov's diameter (12) and Spektor's chord (12) methods. Twenty to thirty TEM micrographs were examined on average for each cure condition. The volume fractions of the dispersed phase obtained by the two methods were in good agreement (9).

Dynamic Mechanical Analysis

The use of an automated torsional braid analysis (TBA) instrument to study cure behavior and its relationship to the properties of the cure state involved obtaining the dynamic mechanical properties of composite specimens, each formed by impregnating a braid substrate with a reactive epoxy resin (9). For the present report, the TBA instrument was used as a conventional freely decaying torsional pendulum (TP) (13) to obtain the quantitative values of shear modulus (G') and logarithmic decrement (Δ) of film specimens ($\sim 0.8 \times 3.0 \times 60$ mm), which had been machined from the large casting. Dynamic mechanical spectra of the fully cured specimens were obtained, after heating from RT to 200°C, on cooling to -170°C at a rate of 1.5°C/minute. Transitions were identified by the temperatures of maxima (and the associated frequencies, ~ 1 Hz) in the logarithmic decrement. The shear modulus was determined from the natural period (P) and logarithmic decrement (Δ) using the following equation (14):

$$G' = \frac{4\pi^2 I \ell}{NP^2} \left(1 + \frac{\Delta^2}{4\pi^2} \right) - \frac{mgb^2}{12N} \quad (1)$$

in which the form factor

$$N = \frac{a^3 b}{3} \left(1 - 0.63 \frac{a}{b} \right)$$

where

a, b, ℓ = thickness, width ($a < b/3$), and length of the specimen, respectively

I = moment of inertia of the oscillating parts of the pendulum

m = mass supported by the specimen (32 gm)

Δ = $\ln (A_i/A_{i+1})$ (A_i is the amplitude of the i th oscillation of a freely damped wave).

Uniaxial Compression Experiments

The true yield stress and yield strain, and the true compressive modulus were determined from uniaxial compression experiments since highly crosslinked epoxy materials fracture prior to plastic yielding when tested under uniaxial tension (6,7). Compression rods ($\ell/d = 1.8$: length = 12.6 mm, diameter = 7 mm) were machined from rods ($\ell \sim 60$ mm). After annealing, the rods were deformed in a compression cage (which had been lubricated with molybdenum disulphide grease) between lightly polished steel plates, at a constant

crosshead displacement rate (1 mm/minute) over a range of temperatures (-90 to 140°C). The true stress, σ , was determined from the following equation (7):

$$\sigma = \frac{P}{A_0} (1 - e) \quad (2)$$

where P = load from the load-displacement record
 A_0 = initial cross-sectional area of specimen
 e = nominal strain from the crosshead displacement after correction for machine deflection using a steel specimen.

Fracture Experiments

The fracture behavior of the cured epoxy materials was examined using compact-tension specimens (100 x 96 x 6 mm) (Figure 1) which had been machined from the large casting. After annealing, a slot was made along the centerline of a specimen using a handsaw and then a sharp crack was formed at the base of the slot by carefully tapping a fresh razor blade in the base thus causing a natural crack to grow for a short distance ahead of the blade. The specimen was mounted in a tensile testing machine (Instron), a constant displacement rate (1 mm/minute) was applied, and the associated load, P , versus displacement was recorded (6,7). Experiments were conducted over a range of temperatures (-90 to 140°C). The value of the fracture energy, G_{IC} (kJm^{-2}), was determined from (15):

$$G_{IC} = \frac{K_{IC}^2}{E} (1 - \nu^2) \quad (3)$$

where K_{IC} = stress intensity factor ($MNm^{-3/2}$)
 E = Young's modulus (GPa) (\equiv initial compressive modulus)
 ν = Poisson's ratio (= 0.40, see later)

and

$$K_{IC} = P_C Q / H / W$$

where P_C = load at crack initiation
 Q = geometric factor
 H = thickness of specimen
 W = width of specimen as defined in Figure 1
 a = crack length

$$[Q = 29.6 (a/W)^{1/2} - 185.5 (a/W)^{3/2} + 655.7 (a/W)^{5/2} - 1017 (a/W)^{7/2} + 638.9 (a/W)^{9/2}].$$

All measurements of K_{IC} are valid according to the procedure and limits prescribed in the relevant American Society for Testing and Materials specification (ASTM E399-72), except at high temperatures starting at approximately 50°C below T_g for each system, which were beyond the recommended limits (16).

After having been fractured at different temperatures, fracture surfaces of the compact-tension specimens were coated with a thin layer ($\sim 600 \text{ \AA}$)

of gold using a high vacuum sputterer for examination by scanning electron microscopy (SEM).

RESULTS AND DISCUSSION

Cure, Transitions and Morphology

The cure process and its relationship to the development of morphology and transitions for the two rubber-modified epoxy systems has been discussed in the previous paper (9). Of the two rubber-modified epoxy systems, the volume fraction of the dispersed phase and values of E_{T_g} for the DTAx16 system were more sensitive to cure conditions. The values of E_{T_g} for the systems studied followed the order: neat (167°C) > DTK-293 (161 to 163°C) > DTAx16 (125 to 148°C). A decrease in E_{T_g} can be a consequence of dissolved rubber but cannot account for the large decrease of E_{T_g} for the present DTAx16 system, which also has the highest volume fraction of dispersed phase. The anomaly for the DTAx16 system has been attributed to the complexity of the cure chemistry which is introduced in using the ATBN rubber (9). In contrast, the cure chemistry for the neat and DTK-293 systems are essentially the same since the reactive end groups in each are identical.

In order to investigate the effect of morphology and E_{T_g} on the mechanical properties, two extreme cure conditions (100°C/40 hr + 170°C/5 hr; and 200°C/3 hr.) were selected in an attempt to provide specimens with the widest variation of properties. The cure conditions, transitions, and details of morphology for these rubber-modified DTK-293 and DTAx16 specimens are tabulated

in Table II, which also includes data for the neat system. The volume fractions of the dispersed phase ranged from about 0.11 for the DTK-293 100°C cured specimen to about 0.34 for the DTAX16 100°C cured specimen, the latter being about 3 times the volume fraction of rubber added initially. The mean diameter of the dispersed phase ranged from about 0.6 μm for the DTK-293 100°C cured specimen to about 3 μm for the DTAX16 100°C cured specimen. The values of $\epsilon T_{g\infty}$ ranged from 125°C for the DTAX16 100°C cured specimen to 163°C for the DTK-293 100°C cured specimen.

The transitions listed in Table II were obtained from torsional pendulum (TP) logarithmic decrement data (Figure 2) using fully cured specimens. For the neat epoxy specimens, three relaxations were observed: a high temperature relaxation associated with $\epsilon T_{g\infty}$; a relaxation at approximately -35°C ($\epsilon T_{\text{sec}\infty}$); and a weak one below $\epsilon T_{\text{sec}\infty}$. For both of the rubber-modified epoxy specimens, four relaxations were observed: a high temperature relaxation associated with $\epsilon T_{g\infty}$; a relaxation at approximately -35°C; a relaxation at about -50°C associated with the rubber glass transition ($R T_g$); and a weak one below $R T_g$. The values of $\epsilon T_{g\infty}$ obtained with the specimens were the same as those obtained using TBA specimens (9). However, the values of $\epsilon T_{\text{sec}\infty}$ for the neat specimens and values of $R T_g$ for the rubber-modified specimens obtained in the TP mode appeared to be slightly higher than those obtained using the TBA mode ($\sim 4^\circ\text{C}$).

Shear and Compressive Moduli

The shear modulus (G') versus test temperature for the DTK-293 and the DTAX16 specimens, as well as data for the neat system, are shown in Figures 3

and 4, respectively. The corresponding compressive modulus versus test temperature plots are shown in Figures 5 and 6, respectively. [The compressive modulus data at the lowest temperature may be unreliable because of severe frictional effects (17).] For elastic isotropic materials, the shear modulus (G') is related to Young's modulus (\equiv compressive modulus) by (18):

$$E = 2G'(1 + \nu) \quad (3)$$

where ν = Poisson's ratio.

The ratio of the compressive to shear moduli was generally found to be about 2.8; consequently Poisson's ratio was taken to be 0.4, which is similar to reported values for other glassy polymeric materials (18).

The values of the modulus for all of the systems are expected to be similar below R_{T_g} , but at higher temperatures to reflect the extent of phase separation and the values of $E_{T_g^\infty}$. In general, between R_{T_g} and $E_{T_g^\infty}$ the moduli of the rubber-modified specimens were lower than those for the neat specimens. The moduli for the 100 and 200°C neat specimens were about the same throughout the test temperature range reflecting the identical values of $E_{T_g^\infty}$ for the two specimens. Similarly, the values of modulus for the DTK-293 specimens cured at 100 and 200°C were about the same in consequence of the insensitivity of both $E_{T_g^\infty}$ and the volume fraction of the rubber-rich domains to cure conditions. In contrast, different values of shear and compressive moduli were observed at test temperatures above 80°C for the DTAX16 100 and 200°C cured

specimens in consequence of the very different values of $\bar{g}T_{g\infty}$ for these two specimens.

Yield Stress and Strain

The true uniaxial compressive yield stress versus test temperature for the DTK-293 system and DTax16 system, as well as data for the neat system, are presented in Figures 7 and 8, respectively. The corresponding yield strain data are shown in Figures 9 and 10, respectively.

The values of yield stress for all the systems decreased with increasing test temperature due to increasing ductility of the matrix. The yield stress and strain behavior for the neat and DTK-293 specimens were insensitive to differences in their previous cure history. In contrast, differences were observed at high temperatures between the DTax16 100 and 200°C cured specimens. In general, the values of yield stress decreased in the order: neat > DTK-293 100°C \cong 200°C > DTax16 200°C > DTax16 100°C which is the order of decreasing $\bar{g}T_{g\infty}$ and the inverse order of increasing volume fraction of dispersed phase. The values of yield strain decreased with increasing temperature, and above 0°C appeared to follow the order: DTK-293 > neat > DTax16.

Fracture Behavior

As for other epoxy systems (6), three basic types of crack growth could be identified from the load-deflection curves: at low test temperatures, brittle stable crack growth; at intermediate temperatures, brittle unstable crack growth

(where crack propagation occurred intermittently in a "stick/slip" manner); and at higher temperatures, ductile stable crack growth.

The fracture energy (G_{IC}) for the systems versus test temperature are shown in Figure 11. For the neat system, the properties of the 100 and 200°C fully cured specimens would be anticipated to be independent of their cure histories since E_{Tg} was not affected by the time-temperature reaction path of cure. It is therefore not surprising that the values of fracture energies for the neat 100 and 200°C cured specimens were the same. The fracture energies for the two DTK-293 specimens (100 and 200°C) also appeared to be insensitive to their cure histories which is attributed to the similar values of E_{Tg} and volume fractions of dispersed phase for these specimens. In contrast, the fracture energies for the DTAx16 specimens (100 and 200°C) were dependent on their cure histories as a consequence of the cure chemistry and volume fraction of dispersed phase of this system being dependent on the time-temperature path of cure (9). The fracture energy of the DTAx16 100°C cured specimen, which has a higher volume fraction of dispersed phase and lower E_{Tg} , was higher than that for the 200°C cured specimen at all temperatures.

A small improvement of fracture energy above that of the neat specimens was observed for the DTK-293 specimens throughout the test temperature range. On the other hand, a larger improvement of fracture energy was observed for the DTAx16 specimens, especially at high temperatures. The fracture energies for the rubber-modified specimens followed the order of increasing volume fraction of the dispersed phase (i.e. DTAx16 100°C > DTAx16 200°C > DTK-293 100°C ≅ 200°C), which is also the decreasing order of values of E_{Tg} (i.e., DTAx16 100°C

< DTAx16 200°C < DTK-293 100°C \approx 200°C). The ratios of fracture energies for the rubber-modified specimens to that for the neat specimens at room temperature varied from 1.7 for the DTK-293 (100 and 200°C) specimens, and to 3.5 for the DTAx16 200°C cured specimen, and to 3.7 for the DTAx16 100°C cured specimen. Fracture energy has been related to the volume fraction of the dispersed phase by other researchers (5,15,19,20). The similar values of fracture energies for the two DTK-293 specimens (100 and 200°C) suggests that the fracture energy is less sensitive to the domain size (within the range of domain size attained), since the mean diameters of the rubbery domains for these two specimens were different although the volume fractions were about the same (Table II). The distribution of particle size in these materials was unimodal (9). It has been reported that the fracture energy may be dependent on the size distribution of rubber-rich inclusions for bimodal distributions (1,2,20).

The improvement of fracture energy for the rubber-modified epoxy materials is a consequence of the increased extent of energy dissipating deformations occurring in the vicinity of the crack tip during loading (6,7). This is demonstrated by comparing the fractographs of a neat 200°C cured specimen (Figure 12) and a DTK-293 200°C cured specimen (Figure 13), both being fractured at 23°C. The lesser extent of shear deformation in the neat specimen results in a lower fracture energy since shear yielding is a principal source of energy dissipation. For the rubber-modified specimen, the deformation processes can involve multiple plastic shear yielding in the epoxy matrix, void formation (cavitation) either in the domain particles or at the particle/matrix interface, and tear of domain material.

The difference in coefficients of thermal expansion between the rubber and the matrix causes the rubber to contract after the particle fails. Cavitation of the rubber gives rise to the appearance of many hollow deep holes in fractographs, some of which (as in Figure 13) appear to have been enlarged by the deformation of the matrix which occurs on fracture. It has been reported that the holes become "hillocks" after swelling the rubber with a solvent indicating that most of the rubber is still in the holes as a lining in the cavities (6). In contrast, fracture surfaces of the DTAx16 100°C cured specimen appear to show fracture of the inclusions without their disappearance; this is attributed to the presence of large amounts of epoxy in the domains (9). Change in the composition of the inclusions may affect fracture energy values (21).

It is noteworthy that the rubber-modified epoxies (i.e. DTK-293 and DTAx16), and nearly all of those reported in the literature, have well-bonded particles as a consequence of the chemical reactivity of the rubber. An attempt was undertaken to investigate the effects of poor bonding by modifying the neat system with the unreacted carboxyl-terminated rubber. Poor interfacial bonding is revealed in the fractograph for the unreacted carboxyl-terminated rubber-modified specimen (Figure 14). The volume fractions for the unreacted carboxyl-terminated rubber-modified specimen and the prereacted carboxyl-terminated rubber-modified DTK-293 specimens were about the same, although the particles for the former specimen were larger. The ratio of fracture energies for the unreacted carboxyl-terminated rubber-modified specimen to that for the neat specimens at room temperature was 1.2, compared to 1.7 for prereacted carboxyl-terminated rubber-modified DTK-293 specimens,

which is an indication of the importance of attaining adequate interfacial bonding. The adverse effects of poor interfacial bonding on the fracture energy would have been displayed more convincingly by using a reacted rubber-modified system which gives has a significant improvement of fracture energy above that of the neat system.

For all of the systems, the fracture energy increased at an accelerating rate with test temperature due to increasing ductility of the matrix. At low temperatures, the crack is relatively sharp and the fracture energy low because the yield stress is high (Figures 7 and 8). Thus the extent of plastic deformation and associated crack tip blunting is relatively limited. As the temperature increases, the yield stress decreases so that more crack tip yielding is possible and the crack becomes blunter. This results in higher failure loads and higher fracture energies at higher temperatures. The increase of ductility of the matrix with temperature is apparent in the fractographs of the DTax16 100°C cured specimens fractured at -60, 0 and 120°C (Figures 15, 16 and 17 respectively).

Since the effect of decreasing T_g is equivalent to the effect of increasing temperature, the fracture energy for the DTax16 100°C specimen should be the highest of all of the specimens due to its low T_g . However, a second factor is the volume fraction of dispersed phase and this specimen also has the highest volume fraction (Table II). The relatively poor improvement of fracture energy for the DTK-293 specimens is a consequence of the similar values of ductility of the neat ($T_g = 167^\circ\text{C}$) and the rubber-modified matrices ($T_g = 161$ and 163°C) and/or the relatively low volume fraction of dispersed phase obtained

using this rubber. In an attempt to investigate further the effect of $T_{g\infty}$ on the fracture energy, comparison of the fracture energies was made by normalizing the test temperature (T) relative to each system's maximum glass transition temperature. The normalized results of G_{IC} versus $[-(T_{g\infty} - T)]$ (Figure 18) clearly show that some of the improvement in G_{IC} for the DTAX16 specimens is due to the increased ductility of the matrix, arising from their lower $T_{g\infty}$ values (compare Figures 11 and 18). However, as would be expected, the volume fraction of the dispersed phase is also playing a role in improving the fracture energy (compare DTK-293 and DTAX16 specimens, Figure 18).

As a caveat, it should be noted that the yield behavior of the matrix is controlled by the details of molecular structure of the matrix. The value of $T_{g\infty}$ is just a convenient "first order" parameter in reflecting the ductility of the matrix.

From the point of view of high T_g matrix materials, the improvement of fracture energy at room temperature by rubber-modification, with the inclusions produced in the present work, is not substantial. For example, at 100°C below $T_{g\infty}$ the maximum improvement over the neat system was about 3 times for the systems studied.

CONCLUSIONS

The mechanical properties of the two fully cured rubber-modified epoxy systems have been investigated versus test temperature as a function of different cure conditions using the neat system as control. The mechanical pro-

erties included shear and compressive moduli, uniaxial yield stress and strain in compression, and the fracture energy (G_{IC}) at a low strain rate. Of the two rubber-modified systems, the mechanical properties of the amino-terminated rubber-modified system were more sensitive to cure history than the prereacted carboxyl-terminated rubber-modified system in consequence of the higher sensitivity of the volume fraction of the dispersed phase and the maximum glass transition temperature ($T_{g\infty}$) of the matrix to cure conditions. (Additional cure reactions are introduced in using the amino-terminated rubber.) The fracture energy increased with temperature (-90 to 140°C) for all of the systems due to increasing ductility of the matrix, in general following the order: amino-terminated rubber > prereacted carboxyl-terminated rubber > neat system. The fracture energies of the different systems were also compared after normalizing the test temperature to the maximum glass transition temperature of each system because of the large variations of $T_{g\infty}$ for the systems [i.e. neat (167°C) > prereacted carboxyl-terminated (161 to 163°C) > amino-terminated rubber (125 to 148°C)]. This procedure clearly revealed that the fracture energy was dependent on both the volume fraction of the dispersed phase and the ductility of the matrix, the latter being related to $T_{g\infty}$.

ACKNOWLEDGMENTS

The authors thank Mr. M. Bennett (Waltham Abbey, U.K.) and Mr. A. Davala (Drexel University, U.S.A.) for their assistance. Chemicals were provided by

the B. F. Goodrich Chemical Co., Ciba-Geigy Chemical Co., Dow Chemical Co.,
Polaroid Corp., and Spencer Kellogg Co. Partial financial support by the
Office of Naval Research is acknowledged.

LITERATURE CITED

1. Sultan, T. N.; McGarry, J. N. Polym. Engr. Sci. 1973, 13 29.
2. Riew, C. K.; Rowe, E. H.; Siebert, A. R. in "Toughness and Brittleness of Plastics"; Deanin, R. D.; Crugnola, A. M., Eds.; ADVANCES IN CHEMISTRY SERIES No. 154, American Chemical Society: Washington, D.C., 1976; p. 326.
3. Bucknall, C. B.; Yoshii, T. Br. Polym. J. 1978, 10, 53.
4. Manzione, L. T.; Gillham, J. K.; McPherson, C. A. J. Appl. Polym. Sci. 1981, 26, 889.
5. Manzione, L. T.; Gillham, J. K.; McPherson, C. A. J. Appl. Polym. Sci. 1981, 26, 907.
6. Kinloch, A. J.; Shaw, S. J.; Tod, D. A.; Hunston, D. L. Polymer 1983, 24, 1341.
7. Kinloch, A. J.; Shaw, S. J.; Hunston, D. L. Polymer 1983, 24, 1355.
8. Kunz-Douglass, S.; Beaumont, P. W. R.; Ashby, M. F. J. Mater. Sci., 1980, 15, 1109.
9. Chan, L. C.; Gillham, J. K.; Kinloch, A. J.; Shaw, S. J. in "Rubber-Modified Thermoset Resins"; Riew, C. K.; Gillham, J. K., Eds.; ADVANCES IN CHEMISTRY SERIES No. 209, American Chemical Society: Washington, D.C., 1984; p. XXX.
10. Riew, C. K., Rubber Chem. Tech. 1981, 54, 374.
11. "Mold Preparation for Araldite Resins, Instruction Manual", Ciba-Geigy Chem. Co., 1972.
12. Underwood, E. E., in "Quantitative Microscopy", DeHoff, R. T.; Rhines, F. N., Eds.; McGraw-Hill: New York, 1968; Chap. 6.
13. Enns, J. B.; Gillham, J. K. in "Computer Applications in Coatings and Plastics"; Provder, T., Ed.; ADVANCES IN CHEMISTRY SERIES No 197, American Chemical Society: Washington, D.C., 1983; p. 329.
14. McCrum, N. G.; Read, B. F.; Williams, G. "Anelastic and Dielectric Effects in Polymeric Solids"; John Wiley and Sons: London, 1967.
15. Kinloch, A. J.; Young, R. J. "Fracture Behavior of Polymers"; Applied Science Publishers: London, 1983.
16. "Plane-Strain Fracture Toughness of Metallic Materials", American Society for Testing and Materials, Philadelphia, 1972; E-399.

17. Hayden, H. W.; Moffatt, W. G.; Wulff, J. "The Structure and Properties of Materials, Volume III, Mechanical Behavior"; John Wiley and Sons: New York, 1975, p. 10.
18. Nielsen, L. E. "Mechanical Properties of Polymers"; Reinhold Publishing Co.: New York, 1962.
19. Pearson, R. A.; Yee, A. F. Polym. Prepr., Am. Chem. Soc., Div. Polym. Mat.: Sci. Engr. 1983, 49, 316.
20. Hunston, D. L.; Kinloch, A. J.; Shaw, J.; Wang, S. S. in "International Symposium on Adhesive Joints"; Amer. Chem. Soc., Kansas City, Sept. 1982, (to be published by Plenum Press, New York, 1984; Mittal, K. L., Ed.).
21. Sayre, J. A. Kunz, S. C.; Assink, R. A. Polymer Prepr., Am. Chem. Soc., Div. Polym. Mat.: Sci. Engr. 1983, 49, 442.

TABLE CAPTIONS

1. Chemical Formulations of the Neat, DTK-293 and DTax16 Systems.
2. Effect of Cure Conditions on Transitions and Morphology.

FIGURE CAPTIONS

1. Dimensions of Compact-Tension Specimen used for Fracture Experiments.
2. Torsional Pendulum (TP) Thermomechanical Spectra for Strip Specimens:
Logarithmic Decrement vs. Temperature.
3. Shear Modulus vs. Test Temperature (DTK-293 and Neat):
(□) DTK-293 100°C; (+) DTK-293 200°C
(◇) Neat 100°C ; (o) Neat 200°C.
4. Shear Modulus vs. Test Temperature (DTAx16 and Neat):
(□) DTAx16 100°C ; (+) DTAx16 200°C
(◇) Neat 100°C ; (o) Neat 200°C.
5. Compressive Modulus vs. Test Temperature (DTK-293 and Neat):
(□) DTK-293 100°C; (+) DTK-293 200°C
(◇) Neat 100°C ; (o) Neat 200°C.
6. Compressive Modulus vs. Test Temperature (DTAx16 and Neat):
(□) DTAx16 100°C ; (+) DTAx16 200°C
(◇) Neat 100°C ; (o) Neat 200°C.
7. Yield Stress vs. Test Temperature (DTK-293 and Neat):
(□) DTK-293 100°C; (+) DTK-293 °C
(◇) Neat 100°C ; (o) Neat 200°C.

8. Yield Stress vs. Test Temperature (DTAx16 and Neat):
(□) DTAx16 100°C ; (+) DTAx16 200°C
(◇) Neat 100°C ; (o) Neat 200°C.
9. Yield Strain vs. Test Temperature (DTK-293 and Neat):
(□) DTK-293 100°C; (+) DTK-293 200°C
(◇) Neat 100°C ; (o) Neat 200°C.
10. Yield Strain vs. Test Temperature (DTAx16 and Neat):
(□) DTAx16 100°C ; (+) DTAx16 200°C
(◇) Neat 100°C ; (o) Neat 200°C.
11. Fracture Energy (G_{IC}) vs. Test Temperature (DTK-293, DTAx16 and Neat):
(□) DTK-293 100°C; (+) DTK-293 200°C
(*) DTAx16 100°C ; (Δ) DTAx16 200°C
(◇) Neat 100°C ; (o) Neat 200°C.
(...) Data beyond the recommended limits for ASTM E399-72.
12. SEM Micrograph of the Fracture Surface of a Neat 200°C Cured Specimen.
(Fracture Temperature = 23°C). [Crack growth direction from right to left, vertical line is crack arrest/crack re-initiation line (6, 15)].
13. SEM Micrograph of the Fracture Surface of a DTK-293 200°C Cured Specimen.
(Fracture Temperature = 23°C).
14. SEM Micrograph of the Fracture Surface of an Unreacted Carboxyl-Terminated

Rubber-Modified Specimen cured at 200°C for 3 hours.

(Fracture Temperature = 130°C).

15. SEM Micrograph of the Fracture Surface of a DTax16 200°C Cured Specimen.

(Fracture Temperature = -60°C.)

16. SEM Micrograph of the Fracture Surface of a DTax16 200°C Cured Specimen.

(Fracture Temperature = 0°C.)

17. SEM Micrograph of the Fracture Surface of a DTax16 200°C Cured Specimen.

(Fracture Temperature = 120°C.)

18. Fracture Energy vs. Test Temperature Normalized to E_{Tg} (DTK-293, DTax16 and Neat):

(□) DTK-293 100°C; (+) DTK-293 200°C

(*) DTax16 100°C ; (Δ) DTax16 200°C

(◇) Neat 100°C ; (o) Neat 200°C

(...) Data beyond the ASTM recommended limits for ASTM E399-72.

TABLE I. Chemical Formulations of the Neat, DTK-293 and DTax16 Systems

	<u>Neat</u>	<u>DTK-293</u>	<u>DTax16</u>
DER 331	100.0	100.0	100.0
TMAB	41.0	51.0	39.9
K-293	-	42.0	-
ATBNx16	-	-	15.0

The basis for the formulations is as follow:

- 1) Neat System (no rubber): 1 epoxy/1 amine hydrogen
- 2) Rubber-modified systems: a) 15 phr of rubber based on 15 phr of unreacted epoxy; b) 1 mole of K-293 contains 0.44 mole of rubber and 0.56 mole of epoxy; c) 1 free epoxy/1 amine hydrogen: assuming all epoxy end groups in DTK-293 and in DER 331 react with TMAB; and assuming all NH in ATBN rubber (including NH in AEP) and TMAB react with epoxy.

TABLE II. EFFECT OF CURE CONDITIONS ON TRANSITIONS AND MORPHOLOGY

Cure Conditions T _{cure} / Time (°C) / (hr)	Neat				DTK-293			DTAx16		
	E ^T g [∞] (Hz)	E ^T sec [∞] (Hz)	E ^T g [∞] (Hz)	R ^T g (Hz)	\bar{d} (μ m)	V _f	E ^T g [∞] (Hz)	R ^T g (Hz)	\bar{d} (μ m)	V _f
100 / 40 +170 / 5	167	-35	163	-47	0.6	0.11	125	-52	3.1	0.34
	(0.8)	(3.3)	(0.4)	(3.3)	[]	[0.11]	(0.6)	(3.3)	[2.7]	[0.38]
200 / 3	167	-35	161	-50	1.5	0.13	148	-52	1.8	0.15
	(0.4)	(3.3)	(0.6)	(3.3)	[2.9]	[0.14]	(0.8)	(3.3)	[2.7]	[0.17]

Transitions designated by temperature in °C and frequency in Hz (rounded brackets).

\bar{d} = mean diameter by Schwartz-Saltykov's diameter method
[Spektor's chord method in square brackets]

V_f = volume fraction of dispersed phase by Schwartz-Saltykov's diameter method
[Spektor's chord method in square brackets]

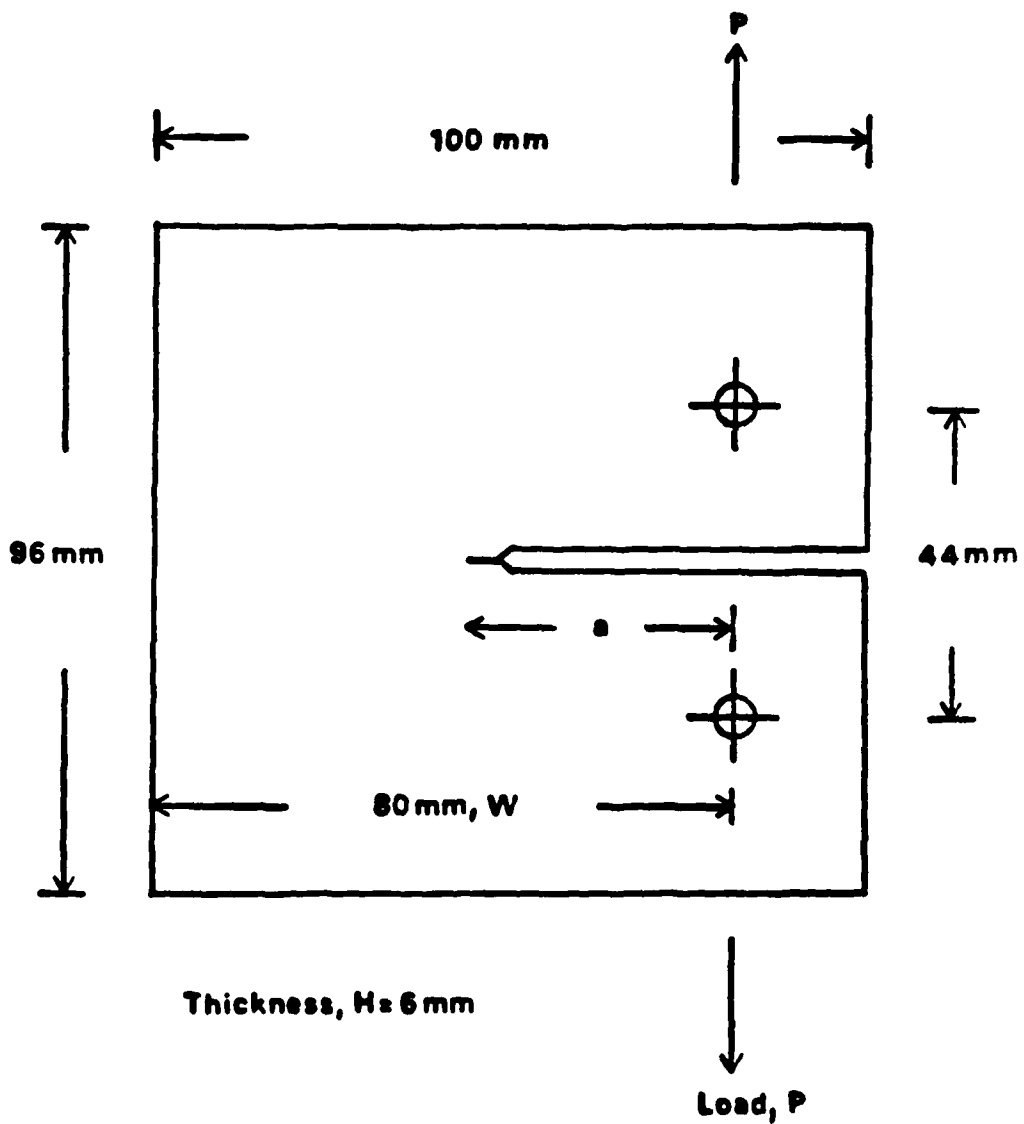


Figure 1

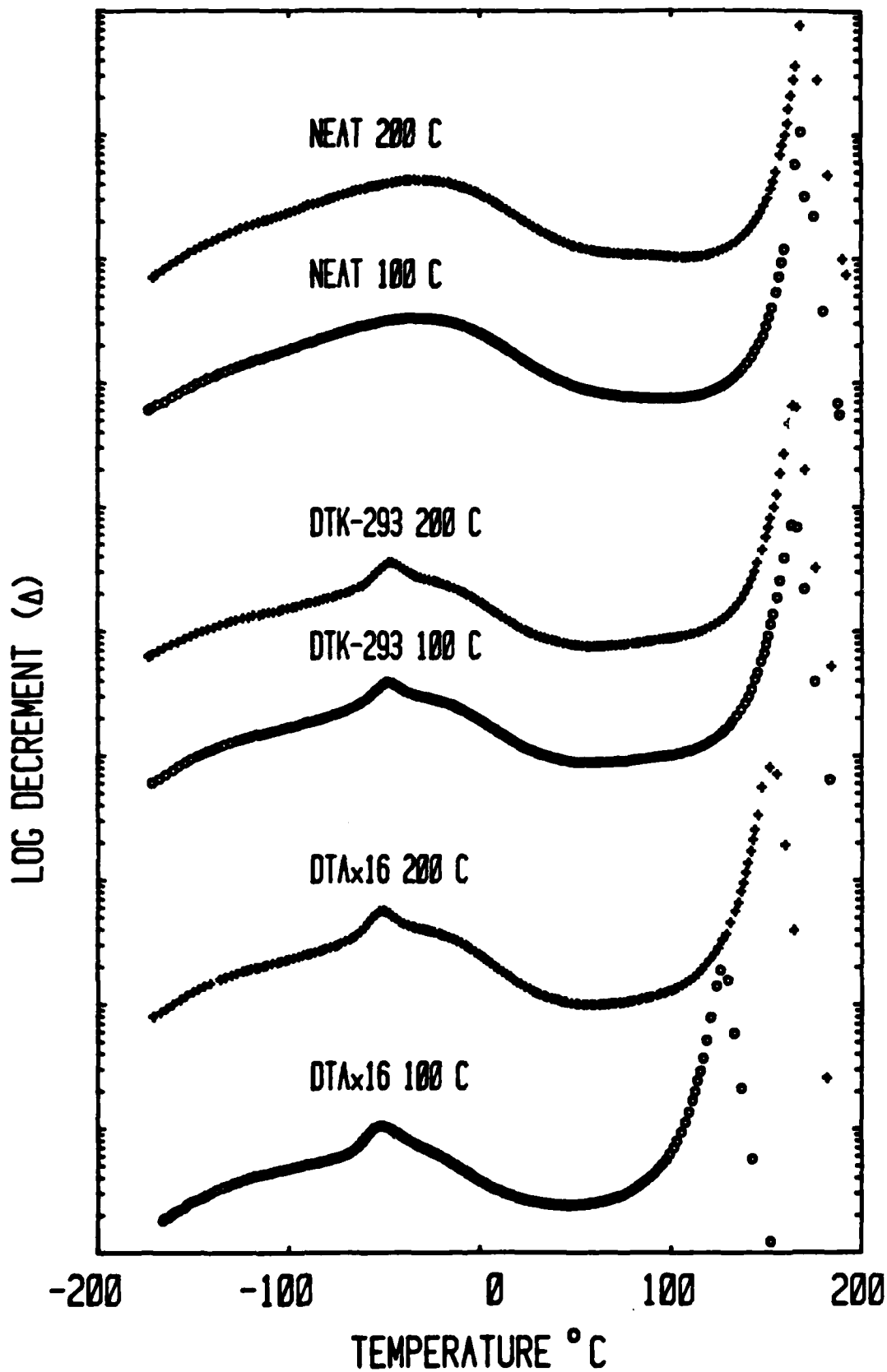


Figure 2

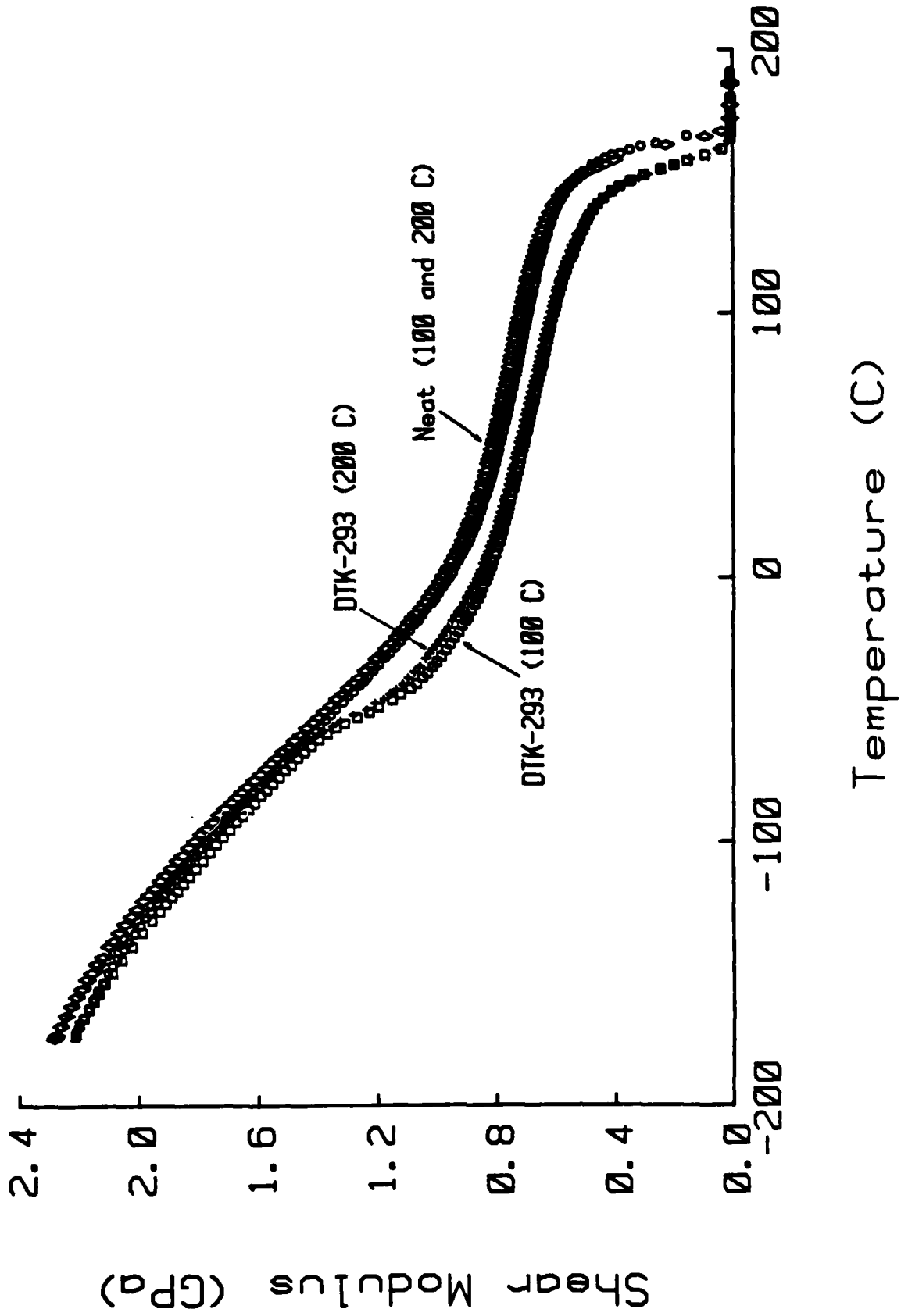


Figure 3

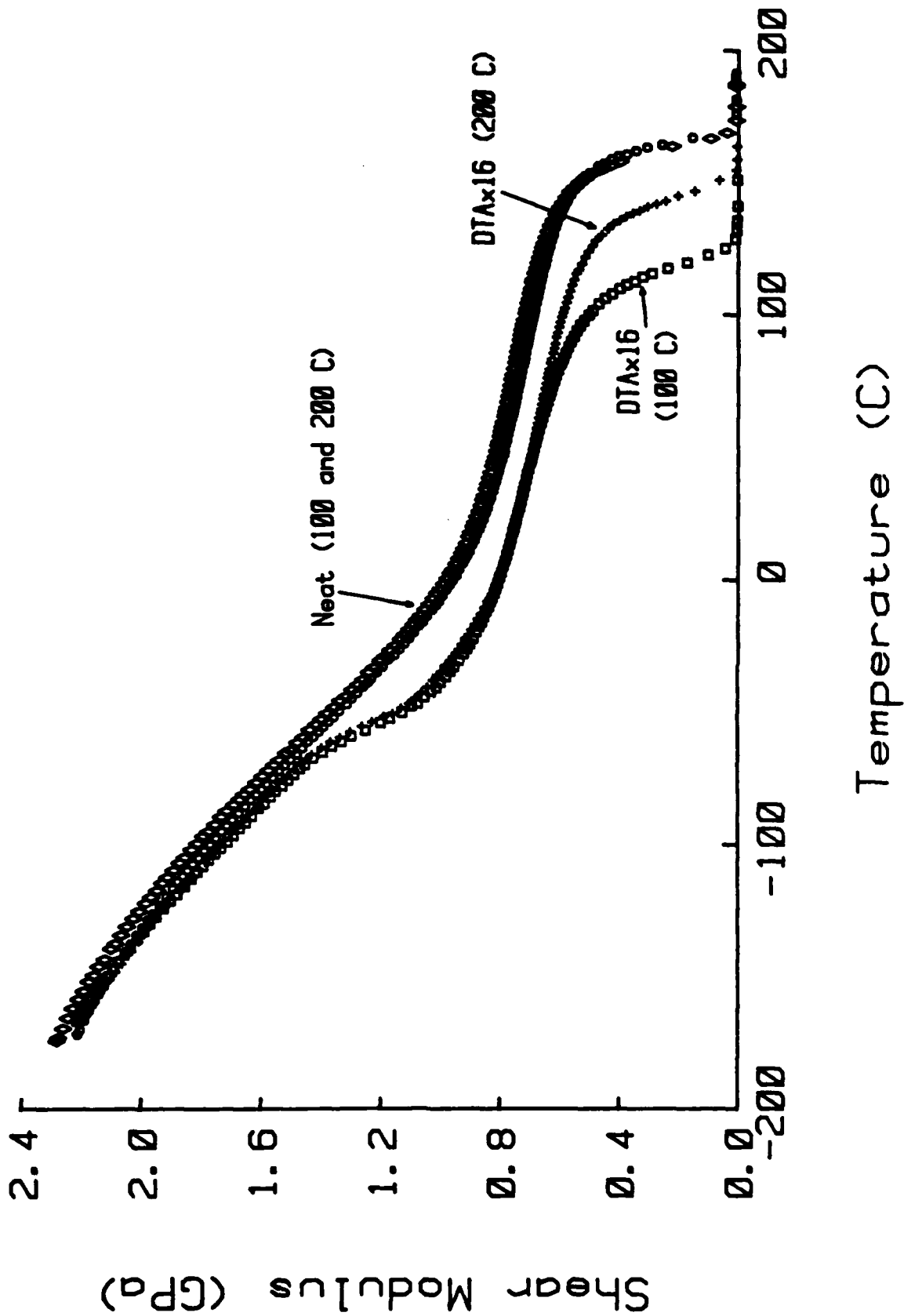


FIG. 4

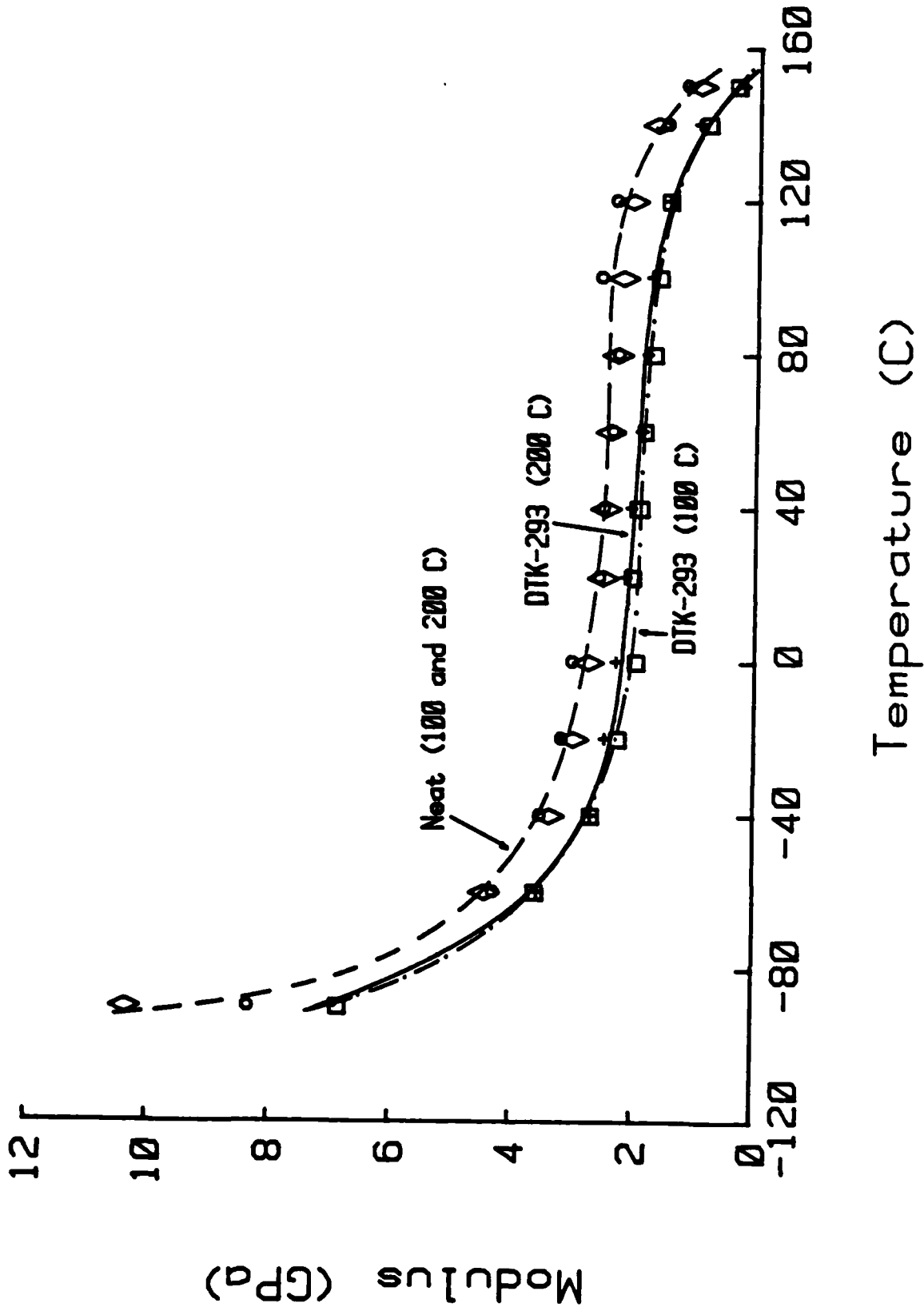


Figure 5

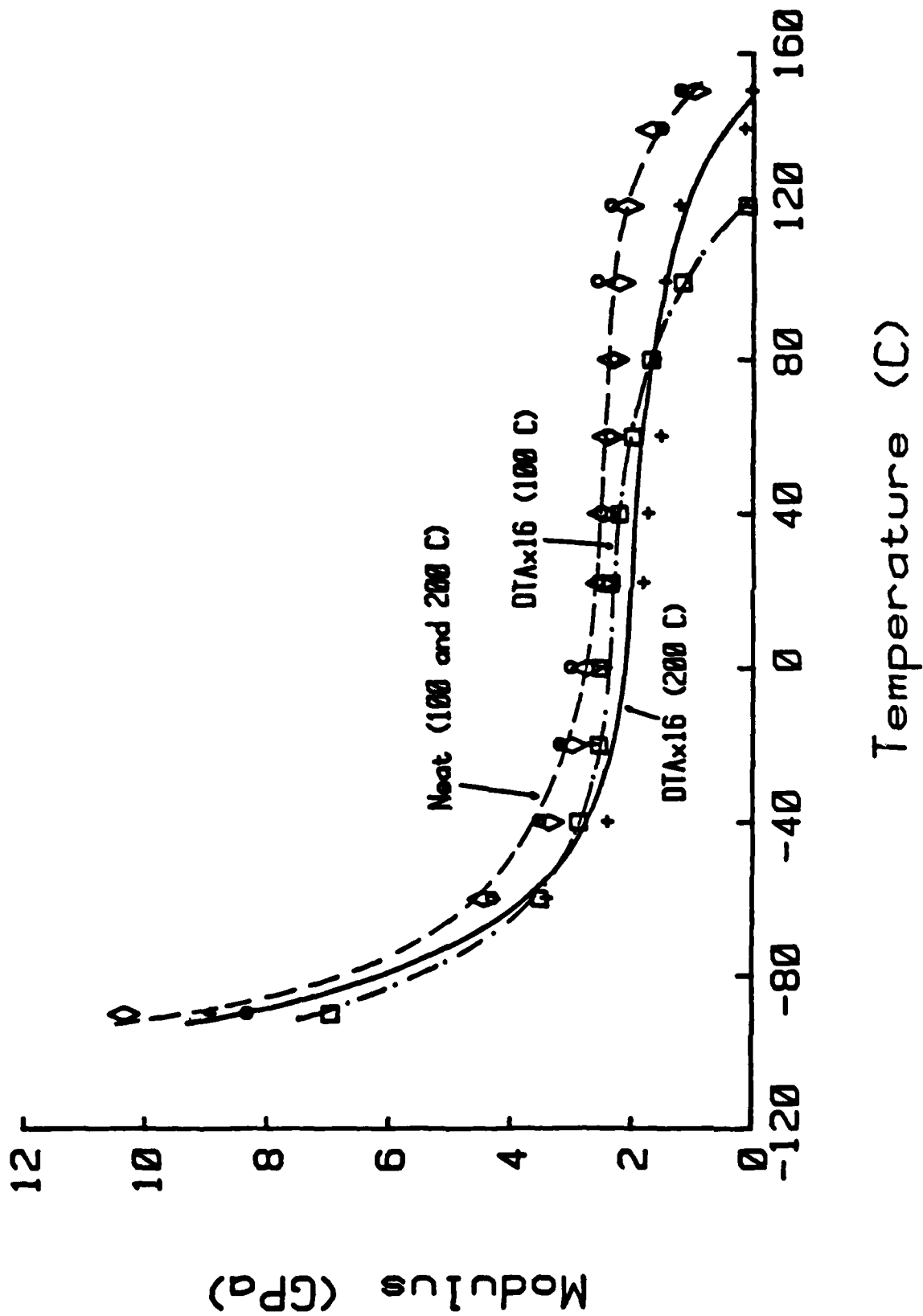


Figure 6

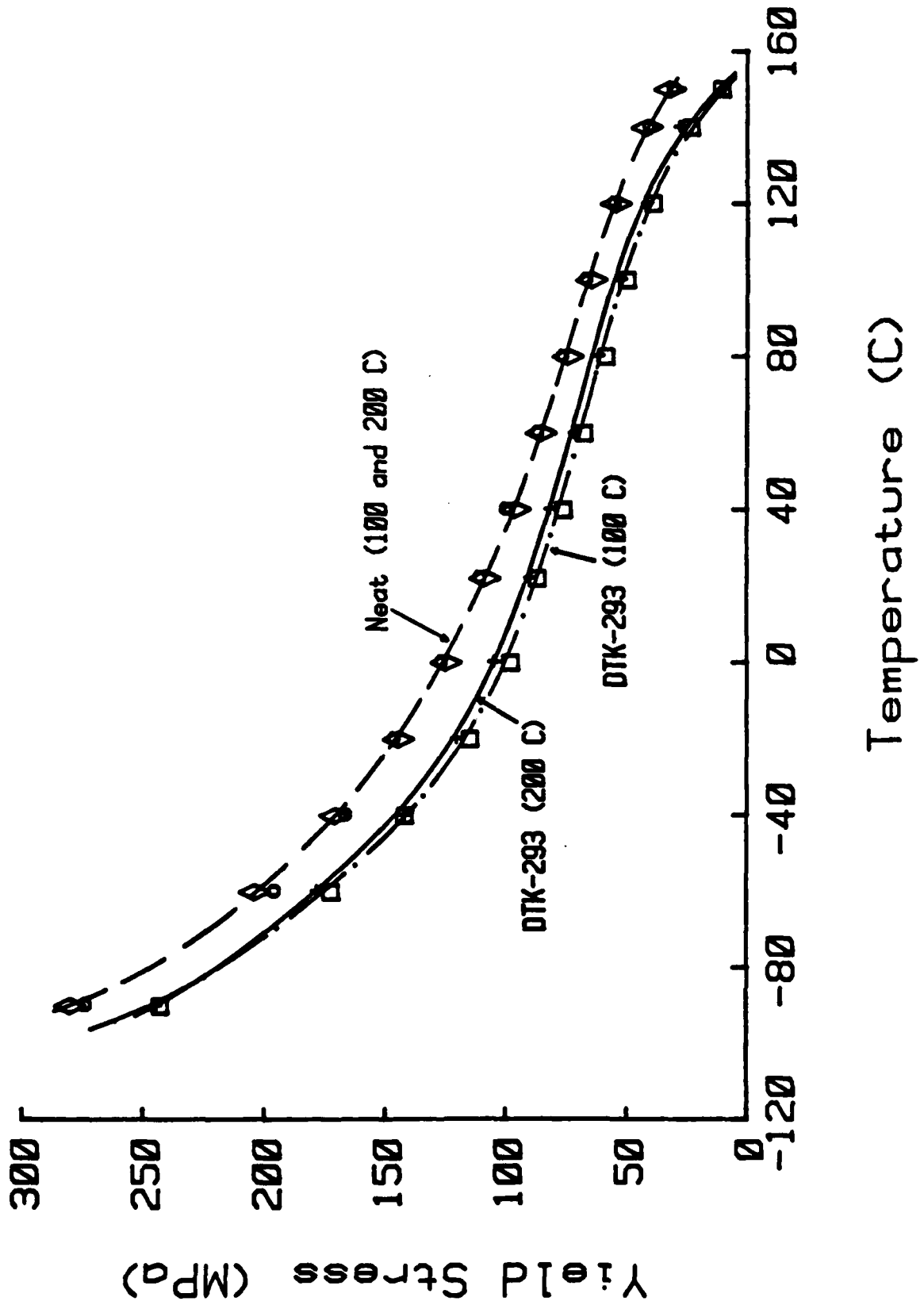


Fig. 7

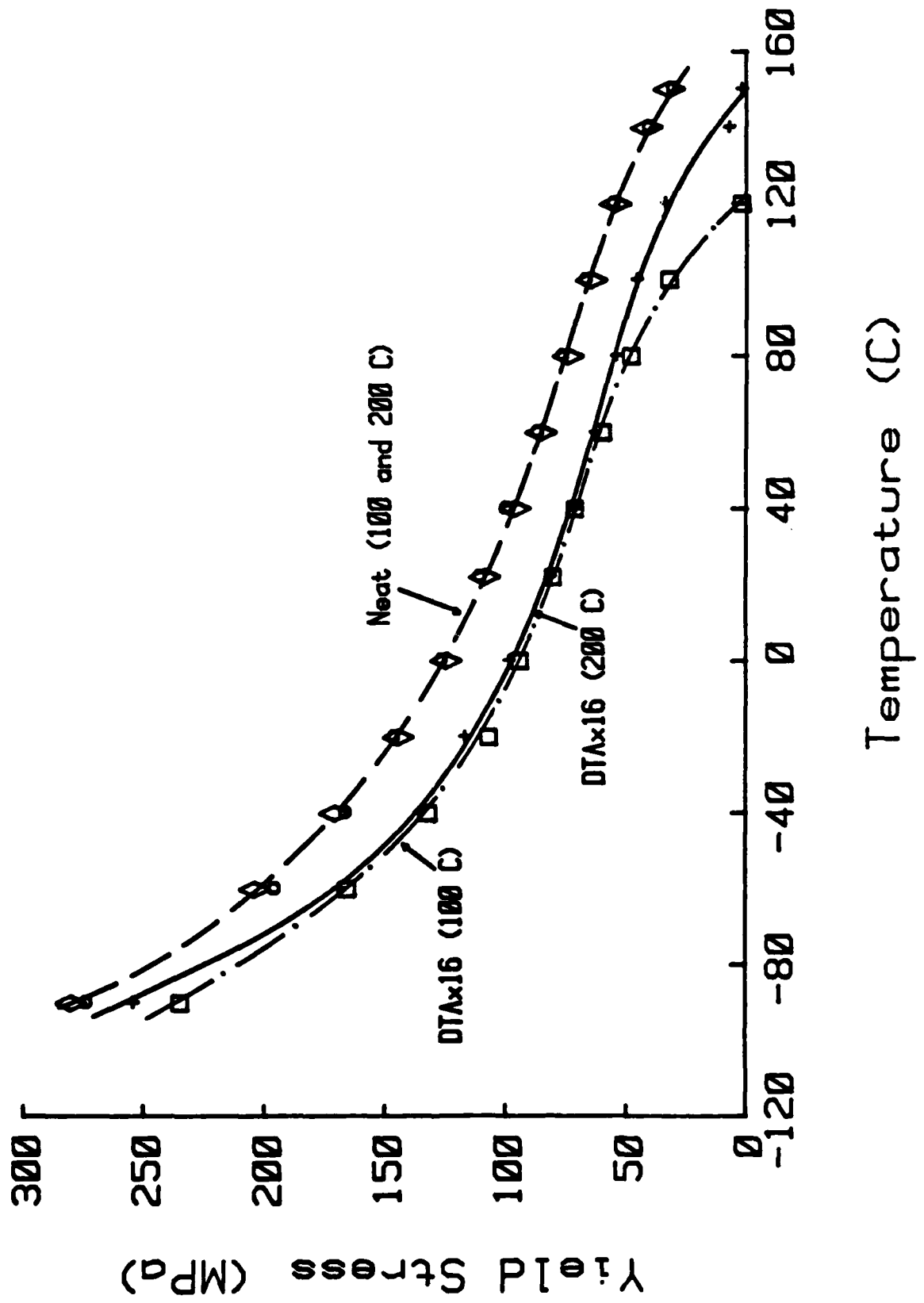


Fig. 8

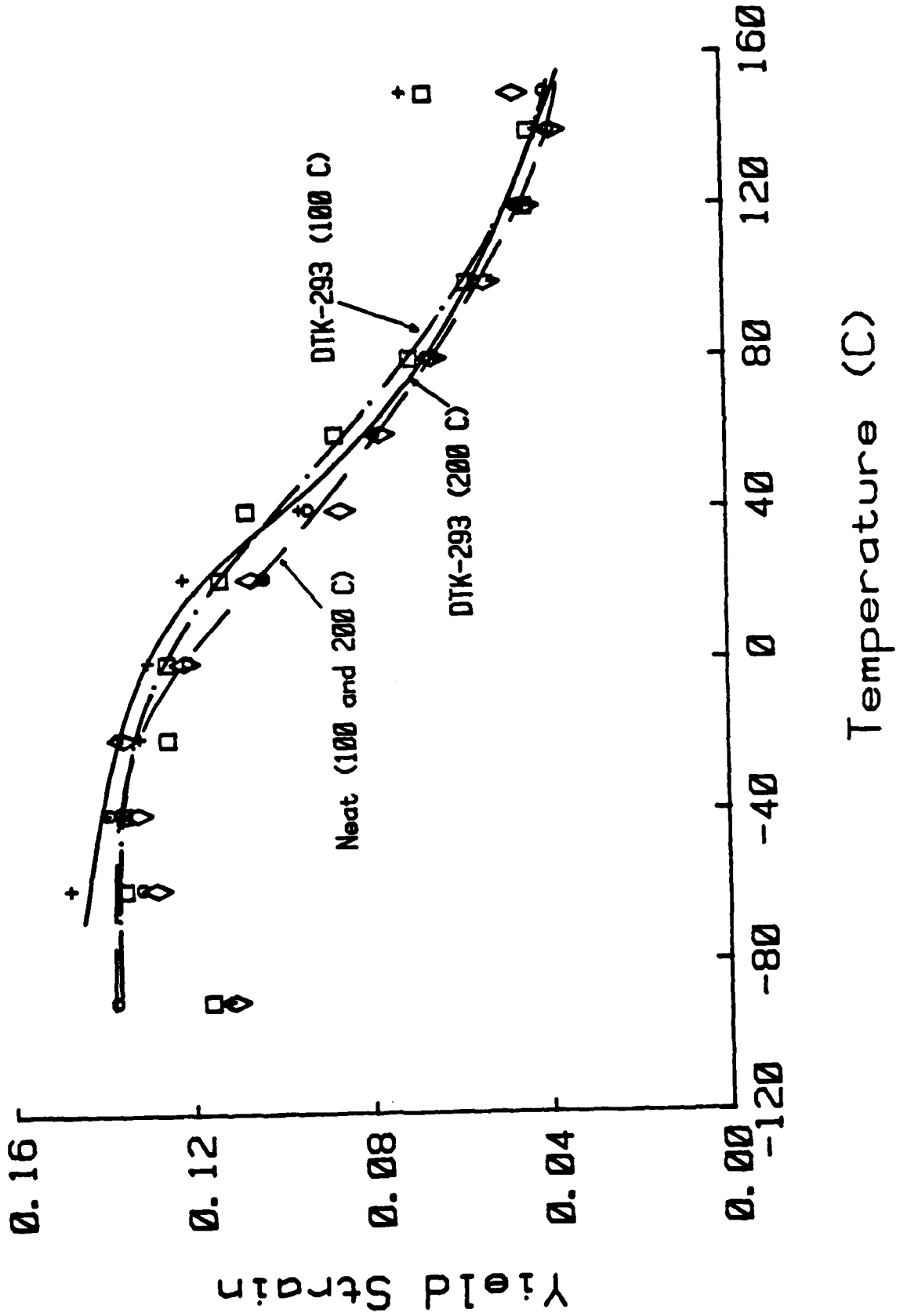


FIG. 9

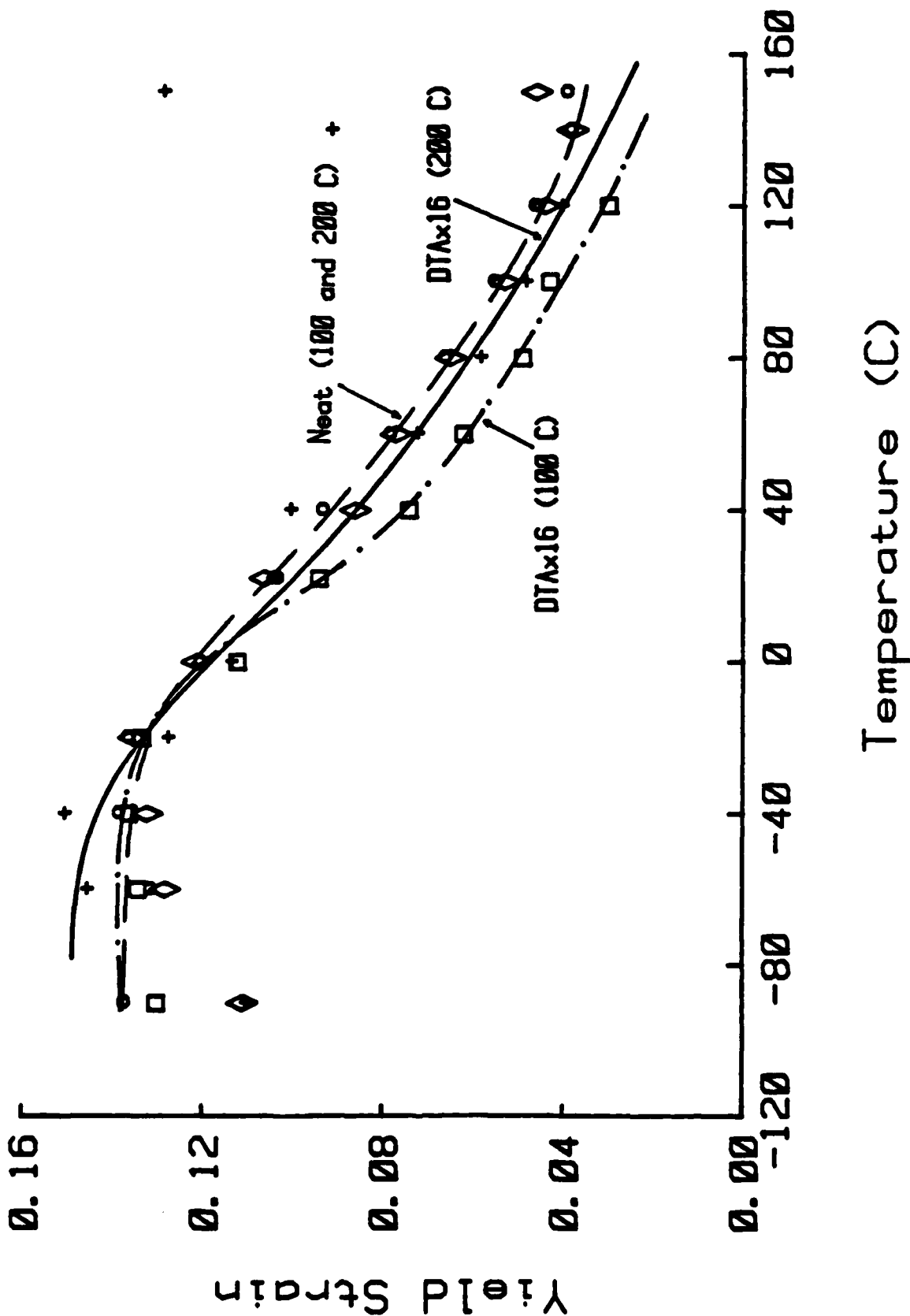


Fig. 10

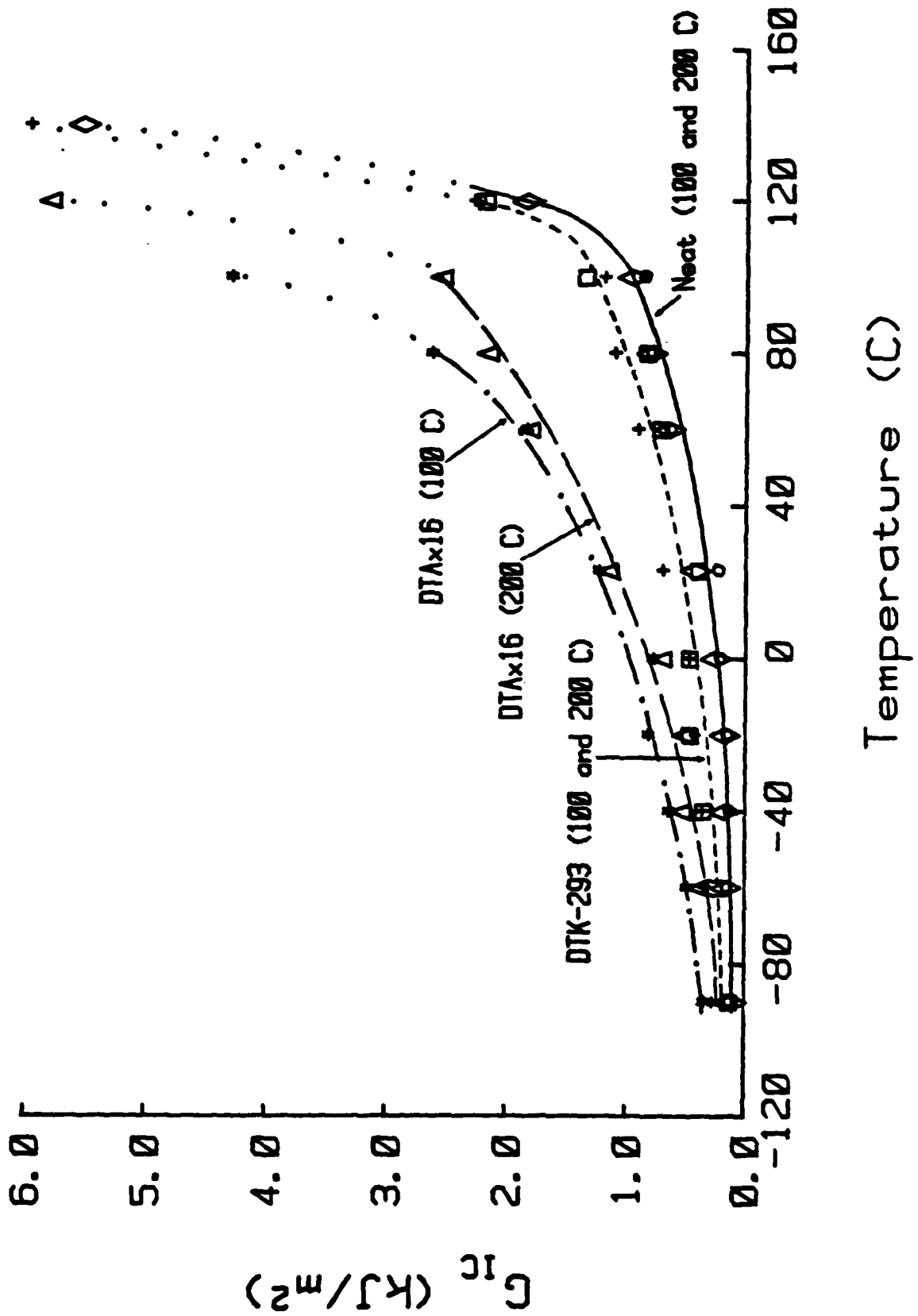


Figure 11

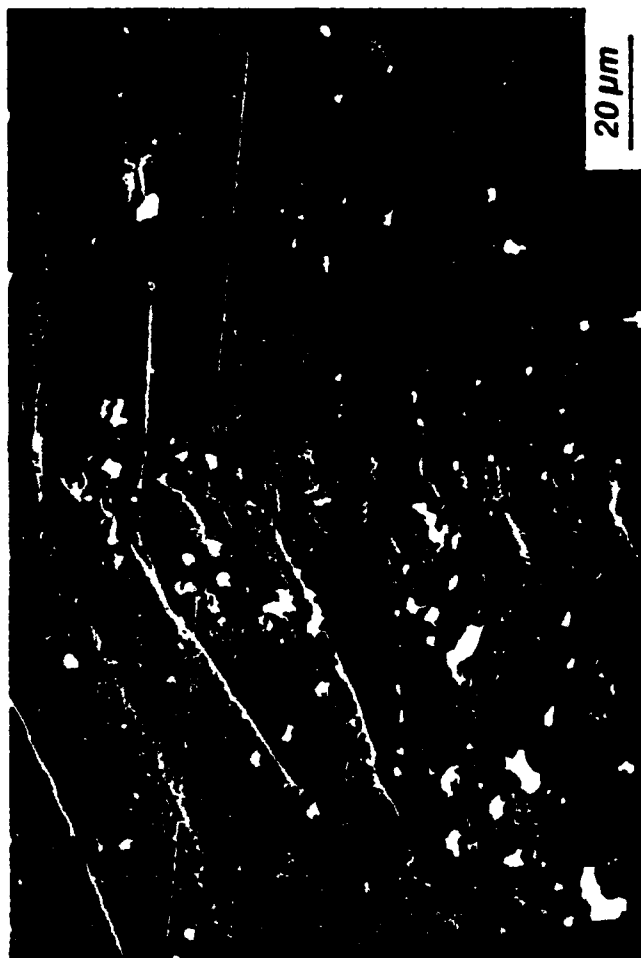


Figure 12



Figure 13



Figure 14



Figure 15

Figure 16





Figure 17

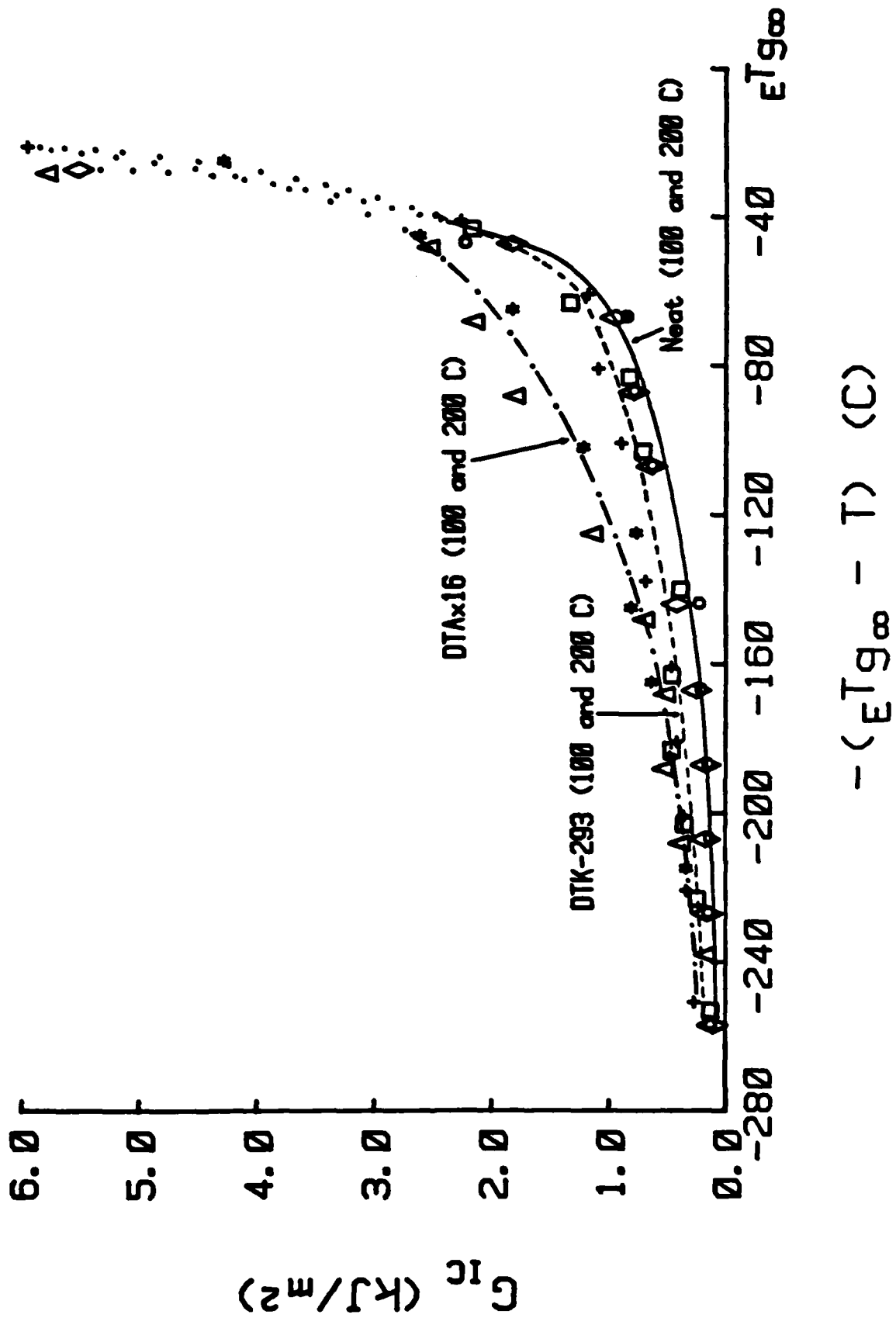


Figure 18

DL/413/83/01
GEN/413-2

TECHNICAL REPORT DISTRIBUTION LIST, GEN

	<u>No. Copies</u>		<u>No. Copies</u>
Office of Naval Research Attn: Code 413 800 N. Quincy Street Arlington, Virginia 22217	2	Dr. David Young Code 334 NORDA NSTL, Mississippi 39529	1
Dr. Bernard Douda Naval Weapons Support Center Code 5042 Crane, Indiana 47522	1	Naval Weapons Center Attn: Dr. A. B. Amster Chemistry Division China Lake, California 93555	1
Commander, Naval Air Systems Command Attn: Code 310C (H. Rosenwasser) Washington, D.C. 20360	1	Scientific Advisor Commandant of the Marine Corps Code RD-1 Washington, D.C. 20380	1
Naval Civil Engineering Laboratory Attn: Dr. R. W. Drisko Port Hueneme, California 93401	1	U.S. Army Research Office Attn: CRD-AA-IP P.O. Box 12211 Research Triangle Park, NC 27709	1
Defense Technical Information Center Building 5, Cameron Station Alexandria, Virginia 22314	12	Mr. John Boyle Materials Branch Naval Ship Engineering Center Philadelphia, Pennsylvania 19112	1
DTNSRDC Attn: Dr. G. Bosmajian Applied Chemistry Division Annapolis, Maryland 21401	1	Naval Ocean Systems Center Attn: Dr. S. Yamamoto Marine Sciences Division San Diego, California 91232	1
Dr. William Tolles Superintendent Chemistry Division, Code 6100 Naval Research Laboratory Washington, D.C. 20375	1		

